Some Properties of the Dissipative Model of Strain-Gradient Plasticity

C Carstensen[1], F Ebobisse[2], AT McBride[3], BD Reddy[⋆,2], P Steinmann[4]

Abstract

A theoretical and computational investigation is carried out of a dissipative model of rate-independent strain-gradient plasticity and its regularization. It is shown that the flow relation, when expressed in terms of the Cauchy stress, is necessarily global. The most convenient approach to formulating the flow relation is through the use of a dissipation function. It is shown, however, that the task of obtaining the dual version, in the form of a normality relation, is a complex one. A numerical investigation of problems in two space dimensions casts further light on the response using the dissipative theory in situations of non-proportional loading. The elastic gap, a feature reported in recent investigations, is observed in situations in which passivation has been imposed. The computational study indicates that the gap may be regarded as an efficient path between a load-deformation response corresponding to micro-free boundary conditions, and that corresponding to micro-hard boundary conditions, in which plastic strains are set equal to zero on all or part of the boundary.

1 Introduction

There has been steady progress in the development of strain-gradient theories of plasticity for over three decades, since the early contribution by Aifantis [1]. The motivation for such theories lies in their ability to capture length-scale dependent effects, which conventional theories are unable to do. Some key works include those by Gao, Huang, Nix and Hutchinson [13, 14], who argue for the inclusion of gradients of plastic strain as a way of accounting for geometrically necessary dislocations, and Fleck and Hutchinson, Gudmundson, and Gurtin and Anand [7, 15, 16], who develop such theoretical models.

This work concerns the small-strain, rate-independent theory of strain-gradient plasticity. The model is based on that proposed for rate-dependent materials by Gurtin and Anand [16] and

⋆ Corresponding author

[1] Institut für Mathematik, Humboldt-Universität zu Berlin, Unter den Linden 6, D-10099 Berlin, Germany. E-mail cc@math.hu-berlin.de

[2] Department of Mathematics and Applied Mathematics, University of Cape Town, 7701 Rondebosch, South Africa. Email {francois.ebobissebille,daya.reddy}@uct.ac.za

[3] School of Engineering, The University of Glasgow, Glasgow G12 8QQ, United Kingdom. Email andrew.mcbride@glasgow.ac.uk

[4] Chair of Applied Mechanics, University of Erlangen-Nuremberg, Egerlandstr. 5, 91058 Erlangen, Germany. Email paul.steinmann@ltm.uni-erlangen.de

Gudmundson [15], and subsequently developed for the rate-independent case by Reddy and coauthors [20, 21], who also carried out an analysis of well-posedness of the problem. The works by Fleck and Willis [10, 11] present and analyze closely related rate-independent and -dependent theories.

In the models referred to above, gradient effects are accounted for either through their inclusion in the free energy, or in an extension of the flow law, or both. These first two cases are referred to respectively as energetic and dissipative models, and are both present in many treatments of gradient plasticity. They differ substantially though in their implications for the theory. Fleck, Hutchinson and Willis [8], for example, point out that it is particularly in cases of non-proportional loading that the energetic and dissipative models lead to quite distinct behaviour. These authors refer to these respectively as incremental and non-incremental theories: their nomenclature stems from the observation that, for energetic (or incremental) theories it is possible to express increments in the microscopic stresses that form part of the description of the model in terms of increments in plastic strain and strain gradients. On the other hand, at least when expressed in local form in a manner that mimics the classical associative flow law, the dissipative model leads to the expression of microscopic stresses – not their increments – in terms of plastic strain and strain gradient increments. These differences in the models are explored and highlighted in [8] in analyses of two problems that involve non-proportional loading. The main distinguishing feature in the two examples is, in the case of the dissipative theory, an elastic gap: that is, elastic behaviour associated with non-proportional loading following loading into the plastic range. This phenomenon has been further investigated by Fleck, Hutchinson and Willis in [9]. Size effects within a one-dimensional dissipative theory of gradient plasticity due to Anand et al. [2] have been analyzed recently by Chiricotto et al. [4].

Fleck and Willis [12] have carried out an analysis for one of the examples studied in detail in [8, 9], viz. the plane-strain tension problem of a strip subjected to passivation of the lateral boundaries at some stage during the loading process. Their analysis shows the existence of the elastic gap for the dissipative problem, and determines theoretically the manner in which plastic flow resumes. A further important outcome of their analysis is the demonstration that the presence of energetic terms has no effect on the size of the elastic gap. Further recent numerical investigations into the appearance of an elastic gap during non-proportional loading include the works by Bardella and Panteghini [3, 19].

The yield criterion and associative flow law for the strain-gradient problem gives the plastic strain-rate (or increment) and its gradient in terms of a normality condition that involves the yield function as a function of the microscopic stresses. Unlike the Cauchy stress these are not known a priori in terms of current displacement and plastic strain and therefore cannot be used to determine whether yield has occurred locally, as has been discussed in [10, 11]. It has been shown in [20] however that the microstresses can be eliminated in favour of the Cauchy stress in the flow relation by resorting to a weak or global form of the flow law. This global form is most

directly derived and formulated in terms of the dissipation function. The corresponding elastic region, yield function and normality relation can then be derived in principle from a dualization procedure. Knowledge of the current yield surface would in turn provide information relevant to the existence of an elastic gap, whose occurrence must correspond to the stress state lying inside the current elastic region rather than on the yield surface.

The objective of this work is to explore various aspects of the dissipative strain-gradient theory, with a view to shedding further light on features of the theory that include those explored in [8, 9, 12]. The global nature of the flow relation, at least when formulated in terms of the Cauchy stress, is shown. The task of determining the corresponding global yield function and normality relation is found not to be readily derivable in closed form. Further insight into the global relation is obtained by analyzing its discrete form, obtained for example from time-discretization combined with finite element approximation in space. Remarkably, even for the discrete problem it is not possible to find in closed form the yield function corresponding to the discrete dissipation function. Rather, an upper bound for the yield function is obtained. These and related issues are examined in further detail in a numerical study using two examples: biaxial deformation of a thin plate, and extension of a circular cylindrical rod. Both are two-dimensional in nature: this allows for an investigation of some features that are not present in the one-dimensional problems in earlier studies. For example, non-proportional loading is effected through the application of passivation, that is, imposition of zero plastic strain increment on part of the boundary, and the resulting yield surface in the multidimensional stress space is explored.

An interpretation, from a mathematical perspective, of the elastic gap is given by appealing to the expression for the yield function as a maximum, taken over all admissible plastic strain increments, of a function involving the dissipation. Numerically, the elastic gap appears to constitute an efficient transition from stress-strain behaviour corresponding to a micro-free or Neumann boundary condition, to that which is obtained assuming micro-hard or Dirichlet boundary conditions.

The plan of the rest of this work is as follows. We summarize the relevant governing relations in Section 2 and derive the flow law in global form, in terms of the dissipation function and involving the Cauchy stress. A mixed formulation, obtained by introducing an auxiliary variable for the plastic strain gradient, is presented in Section 2.2. Section 3 explores the implications of a regularized theory. The dissipation function is not smooth at the origin, and is approximated in Section 3 by one that is smooth. One consequence is that inequalities corresponding to the flow relations are replaced by local or global equations. In Section 4 time-discretization allows the global flow relation to be formulated as one involving plastic strain increments, and for the problem to be formulated as a minimization problem. Such a formulation is not possible for the original problem. In Section 5 we approach the issue of finding the yield function by replacing the original global problem with its fully discrete approximation, and derive an upper bound for

the corresponding yield function. Section 6 is devoted to the numerical investigation. Finally, Section 7 discusses the key results and observations and their implications.

2 Governing equations and inequalities

The model of strain-gradient plasticity that forms the basis of this study is that proposed by Gurtin and Anand [16], with the specialization to rate-independent plasticity by Reddy [20]. Small strains are assumed. The displacement is denoted by $\mathbf{u}$, the total strain by $\boldsymbol{\varepsilon}$, and the stress by $\boldsymbol{\sigma}$. The strain is decomposed into elastic and plastic components $\boldsymbol{\varepsilon}^e$ and $\boldsymbol{\varepsilon}^p$ according to

$$\boldsymbol{\varepsilon} = \boldsymbol{\varepsilon}^e + \boldsymbol{\varepsilon}^p \,. \tag{2.1}$$

The strain-gradient theory makes provision for a 2nd-order microscopic stress tensor $\boldsymbol{\pi}$ and a 3rd-order microscopic stress $\boldsymbol{\Pi}$. The quantity $\boldsymbol{\pi}$ is symmetric and deviatoric, while $\boldsymbol{\Pi}$ is symmetric and deviatoric in its first two indices, in the sense that $\Pi_{ijk} = \Pi_{jik},\ \Pi_{ppk} = 0$. Here and elsewhere the summation convention on repeated indices is invoked, with partial derivatives denoted by a subscript following a comma.

We define the generalized stress S and plastic strain $\mathsf{\Gamma}$ to be the ordered pairs

$$\mathsf{S} = (\boldsymbol{\pi}, \ell^{-1}\boldsymbol{\Pi}), \qquad \mathsf{\Gamma} = (\boldsymbol{\varepsilon}^p, \ell\nabla\boldsymbol{\varepsilon}^p) \,. \tag{2.2}$$

Here ℓ is a length parameter, and the inner product of the two generalized quantities is denoted by

$$\mathsf{S} \diamond \mathsf{\Gamma} := \boldsymbol{\pi} : \boldsymbol{\varepsilon}^p + \boldsymbol{\Pi} \circ \nabla\boldsymbol{\varepsilon}^p = \pi_{ij}\varepsilon^p_{ij} + \Pi_{ijk}\varepsilon^p_{ij,k} \,.$$

Assuming quasistatic behaviour, the equation of macroscopic equilibrium is given by

$$-\mathrm{div}\,\boldsymbol{\sigma} = \mathbf{b} \,, \tag{2.3}$$

where $\mathbf{b}$ is the body force. In addition, the stress and microscopic stresses are related to each other through the microforce balance equation

$$\mathrm{dev}\,\boldsymbol{\sigma} = \boldsymbol{\pi} - \mathrm{div}\,\boldsymbol{\Pi} \quad \text{or, in index form,} \quad (\mathrm{dev}\,\boldsymbol{\sigma})_{ij} = \pi_{ij} - \Pi_{ijk,k} \,. \tag{2.4}$$

Equations (2.3) and (2.4) are required to be satisfied on the domain Ω. The macroscopic boundary conditions on the problem are

$$\mathbf{u} = \bar{\mathbf{u}} \text{ on } \partial\Omega_u \,, \qquad \boldsymbol{\sigma}\mathbf{n} = \bar{\boldsymbol{t}} \text{ on } \partial\Omega_t \,, \tag{2.5}$$

where $\partial\Omega_u$ and $\partial\Omega_t$ are complementary parts of the boundary $\partial\Omega$ with unit outward normal $\mathbf{n}$, and $\bar{\mathbf{u}}$ and $\bar{\boldsymbol{t}}$ are respectively a prescribed displacement and surface traction. In addition we

assume homogeneous micro-hard and micro-free boundary conditions on complementary parts $\partial\Omega_H$ and $\partial\Omega_F$ of the boundary; that is,

$$\boldsymbol{\varepsilon}^p = \mathbf{0} \text{ on } \partial\Omega_H\,, \qquad \boldsymbol{\Pi}\mathbf{n} = \mathbf{0} \text{ on } \partial\Omega_F\,. \tag{2.6}$$

Of particular interest is the weak form of the microforce balance equation (2.4). For this purpose we introduce the space W of plastic strains, defined by

$$W = \{\mathbf{q} \mid q_{ij} = q_{ji},\ q_{ii} = 0,\ q_{ij} \in L^2(\Omega),\ q_{ij,k} \in L^2(\Omega),\ q_{ij} = 0 \text{ on } \partial\Omega_H\}\,.$$

Taking the inner product of (2.4) with arbitrary $\mathbf{q} \in W$, integrating by parts, and imposing the microscopic boundary conditions (2.6), we obtain the weak formulation

$$\begin{aligned}\int_\Omega \operatorname{dev}\boldsymbol{\sigma} : \mathbf{q}\ dx &= \int_\Omega [\boldsymbol{\pi} : \mathbf{q} + \boldsymbol{\Pi} \circ \nabla\mathbf{q}]\ dx \\ &= \int_\Omega \mathsf{S} \diamond \mathsf{Q}\ dx\,,\end{aligned} \tag{2.7}$$

where $\mathsf{Q} = (\mathbf{q}, \ell\nabla\mathbf{q})$.

Given the free energy ψ, the energy imbalance takes the form

$$\dot\psi - \boldsymbol{\sigma} : \dot{\boldsymbol{\varepsilon}}^e - \boldsymbol{\pi} : \dot{\boldsymbol{\varepsilon}}^p - \boldsymbol{\Pi} \circ \nabla\dot{\boldsymbol{\varepsilon}}^p \le 0\,. \tag{2.8}$$

Since we are concerned in this work with the consequences of a dissipative gradient plasticity formulation we restrict attention to free energy functions of the form[6]

$$\psi = \psi^e(\boldsymbol{\varepsilon}^e) = \tfrac{1}{2}\boldsymbol{\varepsilon}^e : \mathbb{C}\boldsymbol{\varepsilon}^e\,, \tag{2.9}$$

in which the elasticity tensor $\mathbb{C}$ is given, for isotropic materials, by

$$\mathbb{C}\boldsymbol{\varepsilon} = \lambda(\operatorname{tr}\boldsymbol{\varepsilon})\boldsymbol{I} + 2\mu\,\boldsymbol{\varepsilon}\,. \tag{2.10}$$

Here λ and μ are the Lamé parameters, and $\boldsymbol{I}$ is the second-order identity tensor. We note also for future reference that the deviatoric part of this relation is given by

$$\operatorname{dev}\mathbb{C}\boldsymbol{\varepsilon} = 2\mu \operatorname{dev}\boldsymbol{\varepsilon}\,. \tag{2.11}$$

Substitution of (2.9) in (2.8) and the usual Coleman-Noll procedure lead to the elastic relation

$$\boldsymbol{\sigma} = \frac{\partial\psi^e}{\partial\boldsymbol{\varepsilon}^e} = \mathbb{C}\boldsymbol{\varepsilon}^e \tag{2.12}$$

and the reduced dissipation inequality

$$\boldsymbol{\pi} : \dot{\boldsymbol{\varepsilon}}^p + \boldsymbol{\Pi} \circ \nabla\dot{\boldsymbol{\varepsilon}}^p \ge 0 \quad \text{or} \quad \mathsf{S} \diamond \dot{\Gamma} \ge 0\,. \tag{2.13}$$

[6] More generally, one considers a free energy that depends in addition on the plastic strain, the plastic strain gradient and, possibly, hardening internal variables. Details may be found, for example, in [20].

2.1 Flow relation

Based on the reduced dissipation inequality (2.13) we postulate the existence of a yield function f, which is a function of the generalized stress S, and a flow relation that takes the form of a normality law: that is,

$$f(\mathsf{S}) \le 0\,, \tag{2.14a}$$

$$\dot{\mathsf{\Gamma}} = \lambda \frac{\partial f}{\partial \mathsf{S}}\,, \tag{2.14b}$$

$$\lambda \ge 0, \quad f \le 0, \quad \lambda f = 0\,. \tag{2.14c}$$

Equivalently, as shown schematically in Figure 1,

$$\dot{\mathsf{\Gamma}} \diamond (\mathsf{T} - \mathsf{S}) \le 0 \qquad \text{for all } \mathsf{T} \in \mathcal{E} := \{\mathsf{T} \mid f(\mathsf{T}) \le 0\}, \tag{2.15}$$

where $\mathcal{E}$ is the convex elastic region.

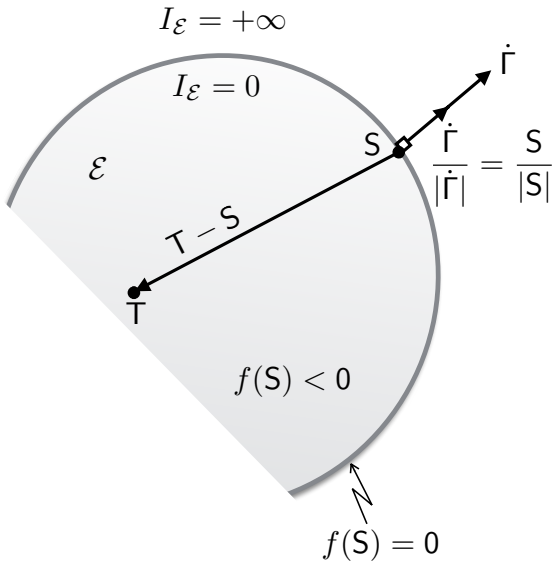

Figure 1: The yield surface and normality relation in generalized stress space

The dissipation function D may be defined using a generalization of the postulate of maximum plastic work in the form

$$D(\dot{\mathsf{\Gamma}}) = \sup\{\mathsf{S} \diamond \dot{\mathsf{\Gamma}} \mid f(\mathsf{S}) \le 0\}\,. \tag{2.16}$$

Note that D is convex and positively homogeneous, the latter being defined as $D(\alpha\dot{\mathsf{\Gamma}}) = |\alpha| D(\dot{\mathsf{\Gamma}})$ for any real number α.

145 **Example** For the special but important case in which

$$f(\mathsf{S}) = |\mathsf{S}| - Y = \sqrt{|\boldsymbol{\pi}|^2 + \ell^{-2}|\boldsymbol{\Pi}|^2} - Y \leq 0, \tag{2.17}$$

146 where Y is the yield stress, it follows from (2.14b) that at yield ($f = 0$)

$$\lambda = |\dot{\mathsf{\Gamma}}| = \sqrt{|\dot{\boldsymbol{\varepsilon}}^p|^2 + \ell^2 |\nabla \dot{\boldsymbol{\varepsilon}}^p|^2}\,.$$

147 Furthermore, for non-zero $\dot{\mathsf{\Gamma}}$,

$$\frac{\dot{\mathsf{\Gamma}}}{|\dot{\mathsf{\Gamma}}|} = \frac{\mathsf{S}}{|\mathsf{S}|} \quad \Longleftrightarrow \quad \mathsf{S} = Y \frac{\dot{\mathsf{\Gamma}}}{|\dot{\mathsf{\Gamma}}|}\,. \tag{2.18}$$

148 From (2.16) it is easily seen that for this example

$$D(\dot{\mathsf{\Gamma}}) = Y|\dot{\mathsf{\Gamma}}|\,. \tag{2.19}$$

149 □

150 There is an important duality between the flow relation written in terms of the yield and
151 dissipation functions. To present this we need the notion of the subdifferential ∂F of a convex function F, defined here on a finite-dimensional space X such as $\mathbb{R}^d$ (see Figure 2).[7] Returning

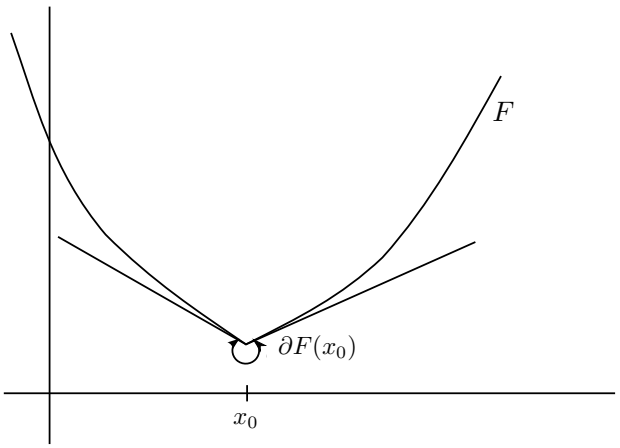

Figure 2: The subdifferential $\partial F(x_0)$ of a convex function F at x_0

152

[7] The subdifferential ∂F of a convex function F is defined by

$$\partial F(\mathbf{x}) = \{\mathbf{p} \mid F(\mathbf{y}) - F(\mathbf{x}) - \mathbf{p} \cdot (\mathbf{y} - \mathbf{x}) \geq 0, \text{ for all } \mathbf{y} \in X\}\,. \tag{2.20}$$

That is, ∂F is the set of tangents at the point $\mathbf{x}$. If F is smooth at $\mathbf{x}$ then ∂F comprises a single member, viz. the tangent $\nabla F(\mathbf{x})$ to F at $\mathbf{x}$, or equivalently the gradient or normal to the level set $F =$ constant. For this and other concepts from convex analysis, see for example [17].

to plasticity, we define the indicator function $I_{\mathcal{E}}$ of a set (in this case the elastic region (2.15)) by

$$I_{\mathcal{E}}(\mathsf{S}) = \begin{cases} 0 & \text{if } \mathsf{S} \in \mathcal{E}\,, \\ +\infty & \text{otherwise}\,. \end{cases} \tag{2.21}$$

This is a convex function. Furthermore, from the definition (2.20) the subdifferential of $I_{\mathcal{E}}$ reads

$$\partial I_{\mathcal{E}}(\mathsf{S}) = \{\dot{\Gamma} \mid \dot{\Gamma} \diamond (\mathsf{T} - \mathsf{S}) \le 0 \text{ for all } \mathsf{T} \in \mathcal{E}\}\,. \tag{2.22}$$

When compared with (2.15) we see that this is simply the *normality relation*, albeit valid for a nonsmooth yield function. We use the notation

$$N_{\mathcal{E}}(\mathsf{S}) \quad \text{for} \quad \partial I_{\mathcal{E}}(\mathsf{S})\,, \tag{2.23}$$

given its geometrical interpretation, and refer to $N_{\mathcal{E}}$ as the normal cone to $\mathcal{E}$ at S. From the definition $N_{\mathcal{E}} = \{\mathsf{0}\}$ if S lies in the interior (that is, the elastic domain) of $\mathcal{E}$: as expected, the generalized plastic strain rate is zero if the generalized stress lies inside the elastic region.

From an important result in convex analysis we have the duality relation

$$\dot{\Gamma} \in N_{\mathcal{E}}(\mathsf{S}) \quad \Longleftrightarrow \quad \mathsf{S} \in \partial D(\dot{\Gamma}). \tag{2.24}$$

The left-hand form of the normality relation has already been established. The equivalence (2.24) and the definition (2.20) indicate that it may also be written as

$$D(\mathsf{Q}) - D(\dot{\Gamma}) - \mathsf{S} \diamond (\mathsf{Q} - \dot{\Gamma}) \ge 0\,, \tag{2.25}$$

as depicted in Figure 3. If D is differentiable at $\dot{\Gamma}$ then (2.25) reduces to the equation

$$\mathsf{S} = \left.\frac{\partial D}{\partial \mathsf{Q}}\right|_{\mathsf{Q}=\dot{\Gamma}} \tag{2.26}$$

(replace Q by $\dot{\Gamma} \pm \epsilon\mathsf{Q}$ and take the limit $\epsilon \to 0$).

Two important examples of dissipation functions are

$$D_1(\dot{\Gamma}) := Y\left[|\dot{\boldsymbol{\varepsilon}}^p| + \ell|\nabla\dot{\boldsymbol{\varepsilon}}^p|\right] \tag{2.27}$$

and

$$D_2(\dot{\Gamma}) := Y|\dot{\Gamma}| = Y\sqrt{|\dot{\boldsymbol{\varepsilon}}^p|^2 + \ell^2|\nabla\dot{\boldsymbol{\varepsilon}}^p|^2}\,. \tag{2.28}$$

The function D_2 corresponds to the definition (2.17) of the yield function. For $\dot{\Gamma} \neq \mathsf{0}$, from (2.26) with $D = D_2$ we recover the relation $(2.18)_2$. Figure 4 shows the level sets corresponding to the dissipation functions D_1 and D_2. It is seen that D_2 is smooth, and so is the corresponding yield function, while D_1 and its corresponding yield function are piecewise smooth.

The dissipation function D_1 is of more than theoretical significance: Evans and Hutchinson [6] have shown that theories based on such a dissipation give results that correlate well with

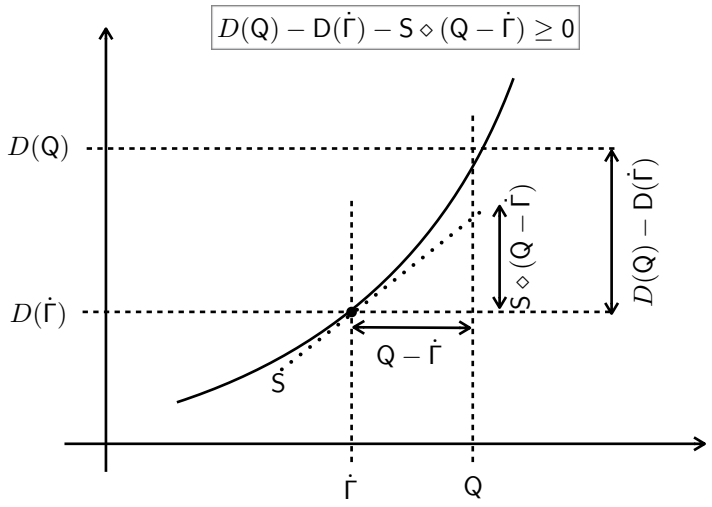

Figure 3: Graphical interpretation of the subdifferential of a convex function D

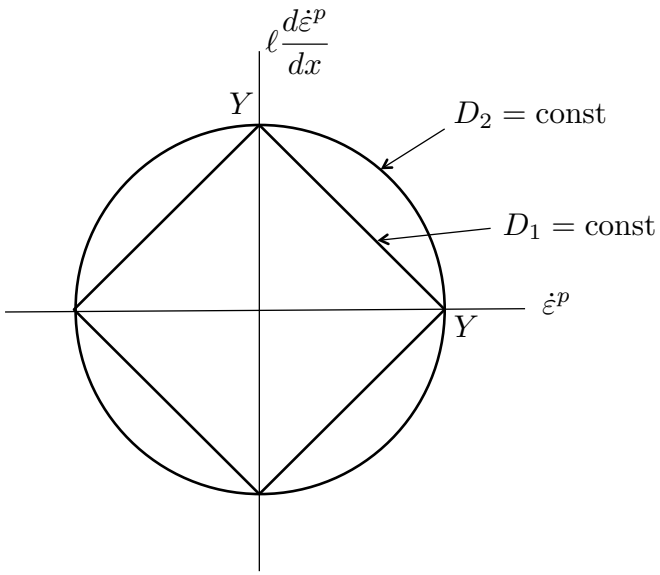

Figure 4: The level sets corresponding to the dissipation functions D_1 and D_2

experiments on bending. The yield function corresponding to D_1 is shown in [20] to be piecewise-smooth or Tresca-like in structure.

We now obtain a weak or global form for the flow relation with a view to eliminating S from it. Integrate (2.25) to obtain

$$\int_\Omega \left[D(\mathsf{Q}) - D(\dot{\Gamma}) - \mathsf{S} \diamond (\mathsf{Q} - \dot{\Gamma}) \right] \, dx \geq 0 \tag{2.29}$$

and add to this the weak form of the microforce balance equation (2.7) to get

$$\int_\Omega \left[D(\mathsf{Q}) - D(\dot{\mathsf{\Gamma}}) - \operatorname{dev}\boldsymbol{\sigma} : (\mathbf{q} - \dot{\boldsymbol{\varepsilon}}^p) \right] \, dx \geq 0 \tag{2.30}$$

or

$$\int_\Omega \left[D(\mathsf{Q}) - D(\dot{\mathsf{\Gamma}}) - \mathsf{\Sigma} \diamond (\mathsf{Q} - \dot{\mathsf{\Gamma}}) \right] \, dx \geq 0 \,, \tag{2.31}$$

where

$$\mathsf{\Sigma} := (\operatorname{dev}\boldsymbol{\sigma}, \mathbf{0}) \,.$$

Concepts such as the subdifferential defined earlier for vectors or tensors at a point (in essence, defined on $\mathbb{R}^d$) have a broader definition that extends to functionals. Thus, if we define the functional

$$j(\dot{\mathsf{\Gamma}}) = \int_\Omega D(\dot{\mathsf{\Gamma}}) \, dx, \tag{2.32}$$

then the subdifferential of j at $\dot{\mathsf{\Gamma}}$ is defined to be the set of functions

$$\partial j(\dot{\mathsf{\Gamma}}) = \left\{ \mathsf{\Sigma} |\ j(\mathsf{Q}) - j(\dot{\mathsf{\Gamma}}) - \int_\Omega \mathsf{\Sigma} \diamond (\mathsf{Q} - \dot{\mathsf{\Gamma}}) \, dx \geq 0 \right\} . \tag{2.33}$$

So we see that (2.31) corresponds to the *global* statement that

$$\mathsf{\Sigma} \in \partial j(\dot{\mathsf{\Gamma}}) \,. \tag{2.34}$$

Furthermore, as in the local case the dual of this relation gives a global normality relation, which we write as

$$\dot{\mathsf{\Gamma}} \in \mathcal{N}_{\mathcal{E}_{\text{glob}}}(\mathsf{\Sigma}) \,. \tag{2.35}$$

The relation (2.35) is equivalent to finding the global form of the normality relation and the corresponding yield function. This is not a trivial task, as we shall see in Section 5.2 where, even for a discrete and therefore finite-dimensional approximation to the problem, at best it is possible to find only an upper bound to the yield function.

Remark Note that the microstress S has been eliminated from the global flow relation. This will be important in interpreting the flow relation for the gradient problem, as the local form (2.14) involves S, which is *indeterminate* in the elastic region.

2.2 A mixed formulation for the dissipation function D_1

If the dissipation function D were a function of two independent variables, it would be feasible to obtain the corresponding yield function and normality law (2.35) by appealing to standard results from convex analysis. The arguments in D are however the plastic strain and its gradient, and this relationship between the two variables complicates the task of finding the yield condition. With this in mind we explore a mixed approach in which the plastic strain gradient is treated as an independent variable.

For convenience we make use of the dissipation function D_1 defined in (2.27), and introduce the auxiliary variable $\mathbf{P}$, a third-order tensor defined by

$$\mathbf{P} = \ell \nabla \boldsymbol{\varepsilon}^p \,. \tag{2.36}$$

The dissipation function is now a function of two independent variables and can be written

$$\begin{aligned} D_1(\boldsymbol{\varepsilon}^p, \mathbf{P}) &:= D_{10}(\boldsymbol{\varepsilon}^p) + D_{01}(\mathbf{P}) \\ &= Y|\boldsymbol{\varepsilon}^p| + Y|\mathbf{P}| \,. \end{aligned} \tag{2.37}$$

The corresponding flow relation reads

$$(\boldsymbol{\pi}, \boldsymbol{\Pi}) \in \partial D_1(\dot{\boldsymbol{\varepsilon}}^p, \dot{\mathbf{P}}) \,. \tag{2.38}$$

Since the two arguments of D_1 are now independent we may use an identity ([5], (Ch. III, eqn (4.17), page 61)) to obtain

$$I_{\mathcal{E}}(\boldsymbol{\pi}, \boldsymbol{\Pi}) = I_{\mathcal{E}_{10}}(\boldsymbol{\pi}) + I_{\mathcal{E}_{01}}(\boldsymbol{\Pi}) \,. \tag{2.39}$$

Here $I_{\mathcal{E}}$ is the indicator function for the set $\mathcal{E}$, $\mathcal{E}_{10} = \{\boldsymbol{\pi} \mid |\boldsymbol{\pi}| \le Y\}$ and $\mathcal{E}_{01} = \{\boldsymbol{\Pi} \mid |\boldsymbol{\Pi}| \le Y\}$. Thus the use of a mixed approach allows the corresponding elastic region to be obtained easily.

The flow relation (2.38) is

$$\int_\Omega D_1(\mathbf{q}, \mathbf{Q}) \; dx - \int_\Omega D_1(\dot{\boldsymbol{\varepsilon}}^p, \dot{\mathbf{P}}) \; dx - \int_\Omega \left[\boldsymbol{\pi} : (\mathbf{q} - \dot{\boldsymbol{\varepsilon}}^p) + \boldsymbol{\Pi} \circ (\mathbf{Q} - \dot{\mathbf{P}}) \right] \; dx \ge 0 \,, \tag{2.40}$$

where $\mathbf{q}$ and $\mathbf{Q}$ are respectively an arbitrary plastic strain and auxiliary variable. Set $\mathbf{q} = \mathbf{q} - \dot{\boldsymbol{\varepsilon}}^p$ in (2.7) and add to (2.40) to obtain

$$\int_\Omega D_1(\mathbf{q}, \mathbf{Q}) \; dx - \int_\Omega D_1(\dot{\boldsymbol{\varepsilon}}^p, \dot{\mathbf{P}}) \; dx - \int_\Omega \left[\boldsymbol{\Pi} \circ [(\nabla \mathbf{q} - \mathbf{Q}) - (\nabla \dot{\boldsymbol{\varepsilon}}^p - \dot{\mathbf{P}})] \right] \; dx - \int_\Omega \operatorname{dev} \boldsymbol{\sigma} : (\mathbf{q} - \dot{\boldsymbol{\varepsilon}}^p) \; dx \ge 0 \,. \tag{2.41}$$

By setting first $\mathbf{Q}$, and then $\mathbf{q}$, equal to zero, we extract the two variational inequalities

$$\int_\Omega Y|\mathbf{q}| \; dx - \int_\Omega Y|\dot{\boldsymbol{\varepsilon}}^p| \; dx - \int_\Omega \boldsymbol{\Pi} \circ \nabla(\mathbf{q} - \dot{\boldsymbol{\varepsilon}}^p) \; dx - \int_\Omega \operatorname{dev} \boldsymbol{\sigma} : (\mathbf{q} - \dot{\boldsymbol{\varepsilon}}^p) \; dx \ge 0 \,, \tag{2.42a}$$

$$\int_\Omega Y|\mathbf{Q}| \; dx - \int_\Omega Y|\dot{\mathbf{P}}| \; dx + \int_\Omega \boldsymbol{\Pi} \circ (\mathbf{Q} - \dot{\mathbf{P}}) \; dx \ge 0 \,. \tag{2.42b}$$

To these must be added the weak form of (2.36), that is,

$$\int_\Omega \mathbf{P} \circ \mathbf{Q} \; dx - \int_\Omega \ell \nabla \boldsymbol{\varepsilon}^p \circ \mathbf{Q} \; dx = 0 \quad \text{for all } \mathbf{Q} \,, \tag{2.43}$$

and the weak form of the equilibrium equation (2.3) together with the boundary conditions (2.5): that is,

$$\int_\Omega \boldsymbol{\sigma}(\mathbf{u}, \boldsymbol{\varepsilon}^p) : \boldsymbol{\varepsilon}(\mathbf{v}) \; dx = \int_\Omega \mathbf{b} \cdot \mathbf{v} \; dx + \int_{\partial \Omega_t} \bar{\boldsymbol{t}} \cdot \mathbf{v} \; ds \,, \tag{2.44}$$

in which the test functions $\mathbf{v}$ satisfy the homogeneous boundary condition $\mathbf{v} = \mathbf{0}$ on $\partial \Omega_u$. We omit details of the (standard) function space setting for the set of weak equations.

Equations (2.42), (2.43) and (2.44) constitute a mixed problem for $\mathbf{u}, \boldsymbol{\varepsilon}^p$, $\mathbf{P}$ and $\boldsymbol{\Pi}$. This appears to be a nonstandard mixed problem.

3 The regularized problem

Later, when developing a computational approach we will focus on the dissipation function D_2, which is an elliptical cone and therefore smooth everywhere except at the origin. It will be convenient to replace D_2 by a regularized approximation $D_{2\eta}$, defined for $\eta > 0$ by

$$D_{2\eta}(\Gamma) = Y\sqrt{|\varepsilon^p|^2 + \ell^2|\nabla\varepsilon^p|^2 + \eta^2}\,. \tag{3.1}$$

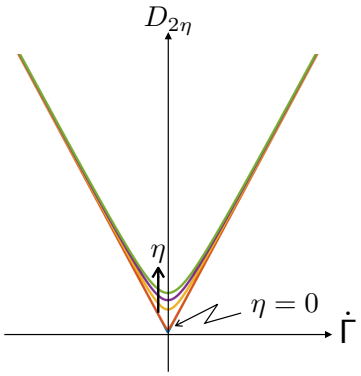

Figure 5: The regularized dissipation function $D_{2\eta}$

The function is shown in Figure 5. The local flow relation corresponding to $D_{2\eta}$ becomes, with the use of (2.26),

$$\mathsf{S} = \nabla D_{2\eta}(\dot{\Gamma}) \quad \Longleftrightarrow \quad \begin{cases} \boldsymbol{\pi} = \dfrac{\partial D_{2\eta}}{\partial \mathbf{q}}\Big|_{q=\dot{\varepsilon}^p} = \dfrac{Y^2\dot{\varepsilon}^p}{D_{2\eta}}\,, \\ \boldsymbol{\Pi} = \dfrac{\partial D_{2\eta}}{\ell\partial\nabla\mathbf{q}}\Big|_{\nabla q=\nabla\dot{\varepsilon}^p} = \dfrac{Y^2\nabla\dot{\varepsilon}^p}{D_{2\eta}}\,. \end{cases} \tag{3.2}$$

Moreover, the inequality (2.29) becomes the equation

$$\int_\Omega \left[\nabla D_{2\eta}(\dot{\Gamma}) - \Sigma\right] \diamond \mathsf{Q}\; dx = 0\,, \tag{3.3}$$

or

$$\int_\Omega \left[\Big(\frac{Y^2}{D_{2\eta}}\dot{\boldsymbol{\varepsilon}}^p - \operatorname{dev}\boldsymbol{\sigma}\Big) : \mathbf{q} + \frac{Y^2}{D_{2\eta}}\ell^2\nabla\dot{\boldsymbol{\varepsilon}}^p \circ \nabla\mathbf{q}\right]\; dx = 0\,. \tag{3.4}$$

Assuming sufficient smoothness, integrating by parts and making use of the boundary conditions (2.6), we obtain the weak equation

$$\int_\Omega \left[\Big(\frac{Y^2}{D_{2\eta}}\dot{\boldsymbol{\varepsilon}}^p - \operatorname{dev}\boldsymbol{\sigma}\Big) - \ell^2\operatorname{div}\Big(\frac{Y^2}{D_{2\eta}}\nabla\dot{\boldsymbol{\varepsilon}}^p\Big)\right] : \mathbf{q}\; dx = 0\,. \tag{3.5}$$

This leads to the pointwise relation

$$\operatorname{dev}\boldsymbol{\sigma} = \frac{Y^2}{D_{2\eta}}\dot{\boldsymbol{\varepsilon}}^p - \ell^2 \operatorname{div}\left(\frac{Y^2\nabla\dot{\boldsymbol{\varepsilon}}^p}{D_{2\eta}}\right). \tag{3.6}$$

We note that $(\operatorname{div}\nabla\dot{\boldsymbol{\varepsilon}}^p)_{ij} = \dot{\varepsilon}^p_{ij,kk}$ and that this quantity is deviatoric if $\dot{\boldsymbol{\varepsilon}}^p$ is. Equation (3.6), which will form the basis of the computational investigation reported in Section 6, could have been obtained directly by substituting the regularized version of the flow relation (3.2) in the microforce balance equation (2.4). Indeed, the first and second terms on the right-hand side of (3.6) correspond respectively to $\boldsymbol{\pi}$ and $-\operatorname{div}\boldsymbol{\Pi}$.

4 A time-discrete minimization problem

The global problem (2.31) does not have an equivalent minimization problem. However, the corresponding time-discrete problem may be posed as a minimization problem. We discretize in time by partitioning the time interval $[0,T]$ as $0 = t_1 < t_2 < \cdots < t_n < \cdots t_N = T$, set $w_n := w(t_n)$ and $\Delta w = w_{n+1} - w_n$ for any function w, and replace the time derivative $\dot{w}$ by its backward Euler approximation $\Delta w/\Delta t$. Then (2.31) becomes

$$\int_\Omega \left[D(\mathsf{Q}) - D(\Delta\Gamma) - \boldsymbol{\Sigma}_{n+1}\diamond(\mathsf{Q}-\Delta\Gamma)\right]\,dx \geq 0\,. \tag{4.1}$$

Here we have multiplied throughout by Δt, made use of the positive homogeneity of D, and replaced the arbitrary $\mathsf{Q}\Delta t$ by Q. Now from (2.11), and noting that $\Delta\boldsymbol{\varepsilon}^p$ is deviatoric,

$$\begin{aligned}\operatorname{dev}\boldsymbol{\sigma}_{n+1} &= \operatorname{dev}\left[\mathbb{C}(\boldsymbol{\varepsilon}_{n+1} - \boldsymbol{\varepsilon}^p_n - \Delta\boldsymbol{\varepsilon}^p)\right]\\ &= \boldsymbol{\sigma}^{\mathrm{tr}} - 2\mu\Delta\boldsymbol{\varepsilon}^p,\end{aligned} \tag{4.2}$$

where

$$\begin{aligned}\boldsymbol{\sigma}^{\mathrm{tr}} &:= \operatorname{dev}\left[\mathbb{C}(\boldsymbol{\varepsilon}_{n+1} - \boldsymbol{\varepsilon}^p_n)\right]\\ &= 2\mu(\operatorname{dev}\boldsymbol{\varepsilon}_{n+1} - \boldsymbol{\varepsilon}^p_n)\end{aligned} \tag{4.3}$$

is a deviatoric trial elastic stress; that is, the deviatoric stress corresponding to purely elastic behaviour in the time step $t_n \to t_{n+1}$. Thus (4.1) becomes

$$\int_\Omega \left[D(\mathsf{Q}) - D(\Delta\Gamma) + 2\mu\,\Delta\boldsymbol{\varepsilon}^p : (\mathbf{q} - \Delta\boldsymbol{\varepsilon}^p) - \boldsymbol{\sigma}^{\mathrm{tr}} : (\mathbf{q} - \Delta\boldsymbol{\varepsilon}^p)\right]\,dx \geq 0\,. \tag{4.4}$$

This is equivalent to the minimization problem

$$\Delta\boldsymbol{\varepsilon}^p = \operatorname{argmin}_{\mathsf{Q}} L(\mathsf{Q}), \tag{4.5}$$

where

$$L(\mathsf{Q}) := \int_\Omega \left[D(\mathsf{Q}) + \mu\,|\mathbf{q}|^2 - \boldsymbol{\sigma}^{\mathrm{tr}} : \mathbf{q}\right]\,dx\,, \tag{4.6}$$

for given $\boldsymbol{\sigma}^{\mathrm{tr}}$ where as before $\mathsf{Q} = (\mathbf{q}, \ell\nabla\mathbf{q})$. Note that, unlike the classical case, this is a global problem which cannot be reduced to a local or pointwise one, given that Q involves $\mathbf{q}$ and its gradient.

5 The spatially discrete problem

5.1 Discrete flow relations

In this section we examine features of the spatially discrete problem. We also discretize in time as in Section 4. The domain, assumed polygonal (in two dimensions) or polyhedral (in three) for convenience, is covered by a mesh comprising

$$\text{NE elements} \quad \text{and} \quad \text{NN nodes} \tag{5.1}$$

where NN excludes those nodes at which the plastic strain is prescribed. The number of plastic strain degrees of freedom at each node is, taking into account the symmetry of $\boldsymbol{\varepsilon}^p$ and the plastic incompressibility condition $\operatorname{tr} \boldsymbol{\varepsilon}^p = 0$,

$$\text{ndofs} = d(d+1)/2 - 1 \tag{5.2}$$

for a d-dimensional problem ($d > 1$).

Denote the global degrees of freedom of $\boldsymbol{\varepsilon}^p$ by p and those of the displacement by d, and assume conventional conforming approximations. Then

$$\boldsymbol{\varepsilon}^p = \mathsf{N}\mathsf{p}\,, \quad \nabla\boldsymbol{\varepsilon}^p = \mathsf{B}\mathsf{p}\,, \quad \mathbf{u} = \overline{\mathsf{N}}\mathsf{d}, \quad \boldsymbol{\varepsilon}(\mathbf{u}) = \overline{\mathsf{B}}\mathsf{d}, \tag{5.3}$$

where N and $\overline{\mathsf{N}}$ are matrices of shape functions and B and $\overline{\mathsf{B}}$ matrices of shape function derivatives.

Here and elsewhere we drop the subscript n that denotes quantities at time t_n.

Since

$$|\boldsymbol{\varepsilon}^p| = \sqrt{\mathsf{p}^T\mathsf{N}^\mathsf{T}\mathsf{N}\mathsf{p}} \qquad \text{and} \qquad |\nabla\boldsymbol{\varepsilon}^p| = \sqrt{\mathsf{p}^T\mathsf{B}^\mathsf{T}\mathsf{B}\mathsf{p}}\,,$$

we have, from (2.27),

$$D_1(\mathsf{p}) = Y\Big[\sqrt{\mathsf{p}^T\mathsf{N}^\mathsf{T}\mathsf{N}\mathsf{p}} + \ell\sqrt{\mathsf{p}^T\mathsf{B}^\mathsf{T}\mathsf{B}\mathsf{p}}\Big], \tag{5.4}$$

which is homogeneous of degree 1 in p. Likewise,

$$\begin{aligned} D_2(\mathsf{p}) &= Y\Big[\sqrt{\mathsf{p}^T\mathsf{N}^\mathsf{T}\mathsf{N}\mathsf{p} + \ell^2\mathsf{p}^T\mathsf{B}^\mathsf{T}\mathsf{B}\mathsf{p}}\Big] \\ &= Y\sqrt{\mathsf{p}^T\mathsf{K}\mathsf{p}}, \end{aligned} \tag{5.5}$$

where the pointwise matrix K is defined by

$$\mathsf{K} = \mathsf{N}^\mathsf{T}\mathsf{N} + \ell^2\mathsf{B}^\mathsf{T}\mathsf{B}\,.$$

Next, set

$$\mathcal{J}_i(\mathsf{q}) := \int_\Omega D_i(\mathsf{q})\,dx \qquad (i = 1, 2); \tag{5.6}$$

then (2.30) becomes, for the incremental problem,

$$\mathcal{J}_i(\mathsf{q}) - \mathcal{J}_i(\Delta\mathsf{p}) - (\mathsf{q} - \Delta\mathsf{p})^T\mathsf{s} \geq 0 \quad \text{for all } \mathsf{q}, \tag{5.7}$$

where the global vector of nodal stresses s is given by

$$\mathsf{s} := \int_\Omega \mathsf{N}^\mathsf{T} \operatorname{dev} \boldsymbol{\sigma}\, dx\,. \tag{5.8}$$

Thus we have the discrete inclusion

$$\mathsf{s} \in \partial\mathcal{J}_i(\Delta\mathsf{p}) \tag{5.9}$$

and the dual of this is, from (2.24),

$$\Delta\mathsf{p} \in N_{\mathcal{E}_i}(\mathsf{s}) \quad \text{or} \quad (\Delta\mathsf{p})^T(\mathsf{t} - \mathsf{s}) \leq 0 \quad \text{for all } \mathsf{t} \in \mathcal{E}_i\,, \tag{5.10}$$

in which $\mathcal{E}_i$ is the elastic region, in the space of discrete stresses s, corresponding to the dissipation function $\mathcal{J}_i$. As with the continuous problem the inclusion (5.9) is equivalent to a minimization problem. First, we have

$$\mathsf{s} = \underbrace{\int_\Omega \mathsf{N}^T\boldsymbol{\sigma}^{\mathrm{tr}}\, dx}_{\mathsf{s}^{\mathrm{tr}}} - \underbrace{\int_\Omega 2\mu\, \mathsf{N}^T\mathsf{N}\, dx}_{\mathsf{M}}\, \Delta\mathsf{p}, \tag{5.11}$$

so that the minimization problem is

$$\Delta\mathsf{p} = \operatorname{argmin}_\mathsf{q} \left(\mathcal{J}_i(\mathsf{q}) + \mathsf{q}^T\mathsf{M}\mathsf{q} - \mathsf{q}^T\mathsf{s}^{\mathrm{tr}}\right). \tag{5.12}$$

Thus we have obtained a vehicle to establish the relation between the dissipation function corresponding to the global dissipation functions $\mathcal{J}_i$ and their corresponding elastic regions $\mathcal{E}_i$.

5.2 Finding the elastic region

We have available the global dissipation functions $\mathcal{J}_i$ and now seek to construct the corresponding elastic regions $\mathcal{E}_i$ and associated yield functions, which would allow the use of the flow law as a normality relation, as in (5.10). Now from a result in convex analysis (see for example [17], page 109), given a dissipation function $\mathcal{J}$, one may construct a yield function $\phi(\mathsf{s})$ as a function of the global nodal stresses with the properties

$$\phi \text{ is positively homogeneous and convex}\,, \tag{5.13a}$$

$$\mathcal{E} = \{\mathsf{s} \mid \phi(\mathsf{s}) \leq 1\}\,, \tag{5.13b}$$

$$\phi(\mathsf{s}) = \sup_{\mathsf{q}\neq 0} \frac{\mathsf{q}^\mathsf{T}\mathsf{s}}{\mathcal{J}(\mathsf{q})}\,. \tag{5.13c}$$

It follows that the yield function can be constructed if we are able to evaluate the supremum in (5.13c).

Locally, the relationship (5.13c) is exemplified in the yield and dissipation functions (2.17) and (2.28). Unfortunately, determining ϕ in (5.13c) corresponding to the *global* functions $\mathcal{J}_i$ is not a simple task, as will be seen: the best that can be done is to obtain a function that is an upper bound for ϕ. To see this, we focus on the dissipation function $\mathcal{J}_2$ and note that this can be written, for constant yield stress Y, as

$$\mathcal{J}_2(\mathsf{q}) = Y \int_\Omega |\mathsf{K}^{1/2}\mathsf{q}| \; dx \,.$$

Taking $|\Omega| = 1$ for convenience we note that

$$\begin{aligned} \mathsf{s}^T\mathsf{q} &= \int_\Omega ([\mathsf{K}(\mathbf{x})]^{-1/2}\mathsf{s})^T([\mathsf{K}(\mathbf{x})]^{1/2}\mathsf{q}) \; dx \\ &\leq \int_\Omega |[\mathsf{K}(\mathbf{x})]^{-1/2}\mathsf{s}| \, |[\mathsf{K}(\mathbf{x})]^{1/2}\mathsf{q}| \; dx \\ &\leq Y^{-1}\big(\max_{\mathbf{x}\in\Omega}|[\mathsf{K}(\mathbf{x})]^{-1/2}\mathsf{s}|\big)\mathcal{J}_2(\mathsf{q}) \,. \end{aligned} \tag{5.14}$$

Hence we have, from (5.13c) and (5.14),

$$\begin{aligned} \phi(\mathsf{s}) &= \sup_{\mathsf{q}\neq\mathsf{0}} \frac{\mathsf{q}^\mathsf{T}\mathsf{s}}{Y\displaystyle\int_\Omega |\mathsf{K}^{1/2}(\mathbf{x})\mathsf{q}| \; dx} \\ &\leq Y^{-1}\max_{\mathbf{x}\in\Omega}|[\mathsf{K}(\mathbf{x})]^{-1/2}\mathsf{s}| \,. \end{aligned} \tag{5.15}$$

We shall now show that the upper bound in (5.15) is not achieved. In order for the expression on the right-hand side of (5.15) to be equivalent to the yield function ϕ, the supremum in the first line of (5.15) has to be achieved at this value. That is, assuming the supremum to be achieved for $\overline{\mathsf{q}} \neq \mathsf{0}$, we must have

$$\frac{\overline{\mathsf{q}}^\mathsf{T}\mathsf{s}}{\displaystyle\int_\Omega |\mathsf{K}^{1/2}(\mathbf{x})\overline{\mathsf{q}}| \; dx} = \max_{\mathbf{x}\in\Omega}|[\mathsf{K}(\mathbf{x})]^{-1/2}\mathsf{s}| \,,$$

or

$$\frac{\displaystyle\int_\Omega ([\mathsf{K}(\mathbf{x})]^{-1/2}\mathsf{s})^T([\mathsf{K}(\mathbf{x})]^{1/2}\overline{\mathsf{q}}) \; dx}{\displaystyle\int_\Omega |\mathsf{K}^{1/2}(\mathbf{x})\overline{\mathsf{q}}| \; dx} = \max_{\mathbf{x}\in\Omega}|[\mathsf{K}(\mathbf{x})]^{-1/2}\mathsf{s}| \,.$$

Since this equation must hold for any s, we require that K be constant, which is a contradiction.

5.3 Illustration of the theory using the problem of a strip in tension

In order to contextualise the theory and to elucidate the numerical results presented in Section 6, we briefly review the study by Fleck, Hutchinson and Willis [8, 9] of a strip in tension that is subjected to passivation on two lateral surfaces at a certain point in its loading history.

The problem is one in plane strain, of a strip $(-\infty \times \infty) \times (-h, h)$ that is subjected to a uniform applied strain $\varepsilon_{11} \equiv \bar{\varepsilon}$ in the x-direction. The only non-zero plastic strain components are ε^p_{11} and $\varepsilon^p_{22} = -\varepsilon^p_{11}$, which follows from plastic incompressibility.

The surfaces $y = \pm h$ are initially traction-free and micro-traction free. At a certain point in the loading history beyond that of initial yield these surfaces are passivated, resulting in the plastic strain rate being zero on the boundaries from this point onwards. The authors in [8] report an *elastic gap*: that is, purely elastic behaviour following passivation, with plastic flow occurring after the load has increased somewhat.

The strain $\varepsilon_{11} = \bar{\varepsilon}$ is prescribed and increases monotonically. We therefore use the time t as a parameter.

The problem in question is one-dimensional, so for definiteness consider a mesh of uniform 1D elements with nodes 1 - 5 located respectively at $x = 0$ and $y = h, h/2, 0, -h/2, -h$ (Figure 6). From symmetry $\mathsf{p}_2 = \mathsf{p}_4$ and $\mathsf{p}_1 = \mathsf{p}_5$.

The uniform phase

For time steps $t_1, t_2, \ldots, t_n$, $\mathsf{p}_1 = \mathsf{p}_5 \neq \mathsf{0}$ and

$$(\mathsf{p}_i)_n \equiv \overline{\mathsf{p}} \quad (i = 1, \ldots 5)\,. \tag{5.16}$$

Assume that the yield stress Y is given. For the case of uniform deformation $\nabla \boldsymbol{\varepsilon}^p = \mathbf{0}$ and the

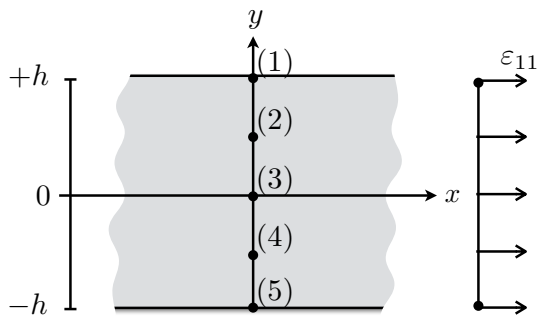

Figure 6: Finite element mesh for the problem of a strip in uniform tension

dissipation and yield functions are the conventional ones.

The passivation phase

Consider the first time step following passivation: we now have $\Delta\mathsf{p}_1 = \Delta\mathsf{p}_5 = \mathbf{0}$ and there are only three free degrees of freedom, corresponding to nodes 2, 3, 4. Each $\Delta\mathsf{p}_i$ has one independent component since there is no shear, and from plastic incompressibility $\varepsilon^p_{22} = -\varepsilon^p_{11}$.

Some insight into the elastic gap may be gained by making use of the definition (5.13c) of the canonical yield function ϕ. Denote by N_{unif} the number of nodal degrees of freedom of plastic

strain: this will be equal to the total number of nodes, since the boundary condition is micro-traction free. Likewise, denote by N_{pass} the number of degrees of freedom in the passivation phase. We have $N_{\text{pass}} < N_{\text{unif}}$ as the plastic strain increment is prescribed to be zero on the boundary nodes. Assuming for convenience that the difference between the vectors s of nodal stresses just before and after initiation of passivation is negligible, it follows from (5.13c) that

$$\begin{aligned}\phi_{\text{pass}}(\mathsf{s}) &= \sup \frac{\mathsf{s}^{\mathsf{T}}\mathsf{q}_{\text{pass}}}{\mathcal{J}(\mathsf{q}_{\text{pass}})} \\ &\leq \sup \frac{\mathsf{s}^{\mathsf{T}}\mathsf{q}_{\text{unif}}}{\mathcal{J}(\mathsf{q}_{\text{unif}})} \\ &= \phi(\mathsf{s}_{\text{unif}}) = 1\,. \end{aligned} \tag{5.17}$$

Here we have denoted by q_{unif} and q_{pass} arbitrary vectors in the uniform and passivated phases, respectively. Also, in the last line we use the assumption that the material is in the plastic range in the uniform phase just before passivation. The inequality in the second line follows from the fact that $\dim \mathsf{q}_{\text{pass}} = N_{\text{pass}} < N_{\text{unif}} = \dim \mathsf{q}_{\text{unif}}$, so that the supremum is being taken over a larger set. From this bound it is clearly possible that $\phi_{\text{pass}} < 1$, so that the response *could be elastic* in the initial passivation phase. That this is the case for this particular problem has been shown theoretically in [12].

When plastic flow does eventually take place, the inclusion (5.9) gives an explicit expression for the stress, viz.

$$\begin{aligned}\mathsf{s}_{n+1} &= \left.\frac{\partial \mathcal{D}}{\partial \mathsf{p}}\right|_{\Delta \mathsf{p}} \\ &= \int_\Omega \frac{\mathsf{K}\Delta\mathsf{p}}{\sqrt{(\Delta\mathsf{p})^T \mathsf{K}\Delta\mathsf{p}}}\, dx\,. \end{aligned} \tag{5.18}$$

Unlike the classical case, it appears not to be possible to obtain a closed-form expression for the inverted form of this expression.

6 Numerical investigation

We consider fully discrete approximations of the problem, based on weak forms of the equilibrium, microforce balance, and flow relations, with time-discretization as set out in Section 4, and making use of the regularized form (3.1) of the dissipation function. Assume that the state of the system is known at time t_n and that a backward Euler time-integration scheme is employed. The weak form of the equilibrium and microforce balances (2.3)–(2.4) for the system at $t_{n+1} = t_n + \Delta t$ (the system of residual equations) are given by

$$R_{\mathsf{d}} := \int_\Omega \boldsymbol{\varepsilon}(\boldsymbol{v}) : \boldsymbol{\sigma}_{n+1}\, dx - \int_{\partial\Omega_t} \boldsymbol{v}\cdot\bar{\boldsymbol{t}}_{n+1}\, ds\,, \tag{6.1}$$

$$R_{\mathsf{p}} := \int_\Omega \boldsymbol{q} : \operatorname{dev}\boldsymbol{\sigma}_{n+1}\, dx - \int_\Omega \boldsymbol{q} : \boldsymbol{\pi}_{n+1}\, dx - \int_\Omega \nabla\boldsymbol{q} : \boldsymbol{\Pi}_{n+1}\, dx\,, \tag{6.2}$$

where as before $\mathbf{v}$ and $\mathbf{q}$ are respectively displacement and plastic strain test functions, $\boldsymbol{\pi}$ and $\boldsymbol{\Pi}$ are given by (3.2), and

$$\boldsymbol{\sigma}_{n+1} = \mathbb{C}(\boldsymbol{\varepsilon}(\boldsymbol{u}_{n+1}) - \boldsymbol{\varepsilon}^{\mathrm{p}}_{n+1}).$$

For convenience we make use of the regularized version (3.1) of the dissipation function, so that the microstresses are given by (3.2). Equation (6.2) thus incorporates both microforce balance and the flow relation, and after discretization is equivalent to the smooth minimization problem (5.12). The magnitude of the perturbation η is chosen to be small enough for trends in the elastic-plastic behaviour to be captured with sufficient accuracy.

It has been shown in [20] that a sufficient condition for the existence of a unique solution to the purely dissipative problem is that there be some hardening present. Accordingly, we introduce a small amount of hardening to avoid pathologies in the numerical solutions; the hardening may be viewed as a small perturbation, which does not affect the overall features of the solutions.

Plastic incompressibility is enforced via the inclusion of the energy term

$$\psi_{\mathrm{inc}} = \frac{\beta}{2}(\operatorname{tr} \boldsymbol{\varepsilon}^p)^2 \,,$$

whose derivative with respect to the vector p is added to R_{p}, where $\beta > 0$ is a penalty.

The problem is then one of solving equations (6.1) and (6.2) for the displacement $\boldsymbol{u}_{n+1}$ and plastic strain increment $\mathsf{d}\boldsymbol{\varepsilon}^p$.

The displacement and plastic strain fields (and their associated test functions) are approximated on a mesh of quadrilateral elements with conforming bilinear interpolations. The vector of global unknowns is denoted by $\mathsf{x} := (\mathsf{d}, \mathsf{p})$. A global Newton–Raphson procedure is used to linearize and iteratively solve the system of residual equations. An arbitrary variable evaluated at the current iteration (i) in time step $n+1$ is denoted by $(\bullet)^{(i)}_{n+1} \equiv (\bullet)^{(i)}$. The linearized problem and the iterative update of the solution vector are then given by

$$\left.\frac{\partial \mathsf{R}}{\partial \mathsf{x}}\right|_{(i)} \cdot \Delta\mathsf{x} = -\mathsf{R}^{(\mathrm{i})} \,,$$
$$\mathsf{x}^{(i+1)} = \mathsf{x}^{(i)} + \Delta\mathsf{x} \,,$$

where $\mathsf{R} := (R_{\mathsf{d}}, R_{\mathsf{p}})$.

The finite element library AceGen [18] is used to implement the finite element interpolation, and to compute the residual and tangent contributions using automatic differentiation. This approach greatly simplifies the implementation. In addition, an adaptive time-stepping algorithm is employed.

We consider two examples, viz. a thin plate is subjected to biaxial deformation, and uniaxial extension of a rod.

6.1 Biaxial deformation of a thin micro-plate

In this example the role of the microscopic boundary conditions on the evolution of the problem are of particular interest. The material properties used in this example and the next are listed in Table 1, unless stated otherwise.

Table 1: Constitutive parameters used for the numerical examples unless stated otherwise

First Lamé parameter	λ	1.05×10^{-1}	N/µm^2
Poisson's ratio	ν	0.3	
Yield stress	Y	1×10^{-3}	N/µm^2
Regularization parameter	η	5×10^{-4}	
Incompressibility penalty	β	1×10^{6}	N/µm^2

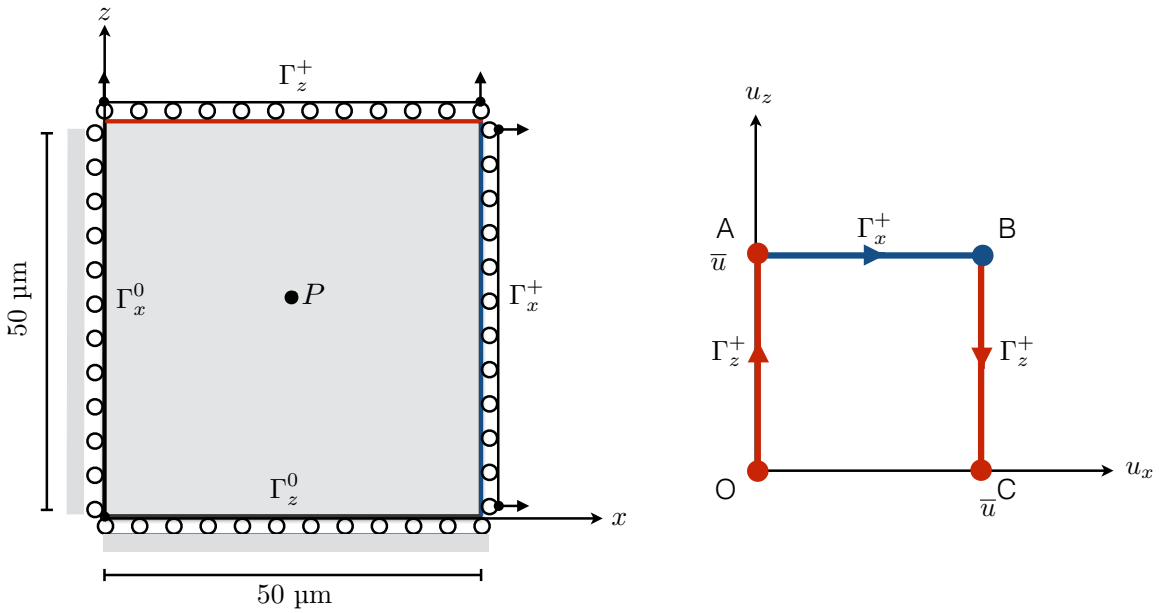

Figure 7: The problem of biaxial deformation in a plate and a schematic of the various stages of loading.

Consider the $50 \times 2 \times 50$ µm plate shown in Fig. 7. The motion of the upper boundary Γ_z^+ and the right boundary Γ_x^+ is defined in three stages. During load stage O–A (see Fig. 7), Γ_z^+ is displaced in the positive z-direction by a distance $\overline{u} = 2/3$ µm while Γ_x^+ is prevented from displacing in the x-direction. During load stage A–B, Γ_x^+ is displaced in the positive x-direction by a distance $\overline{u}$ while Γ_z^+ is prevented from displacing in the z-direction. Finally, during stage B–C, the loading imposed during stage O–A is reversed by displacing Γ_z^+ a distance $-\overline{u}$ in the z-direction, while Γ_x^+ is prevented from displacing in the x-direction. Each loading stage (that

is, OA, AB, BC and CA) corresponds to a time of 0.5 s. The plate is free to displace in the y-direction.

The domain is discretized using 2500 elements with one element through the thickness. The maximum permissible time-step size is 1×10^{-3} s. The length scale is $l = 0.1L$, where $L = 50$ µm.

The influence of a microscopic boundary condition for the plastic strain evolution on the global response is investigated by prescribing Γ_z^+ to be either (a) micro-free, (b) micro-hard from the onset, or (c) micro-free for $0 \leq t < t_{\text{pass}}$, and thereafter preventing the evolution of plastic strain. The boundary condition (c) is termed passivation. When imposed, passivation will occur at time $t_{\text{pass}} = 0.4$ s. The response of a material point in the centre of the specimen $P = [25, 1, 25]$ µm is monitored.

The evolution of the magnitude of the Cauchy stress and stress deviator at the point P for the various microscopic boundary conditions is shown in Fig. 8. The macroscopic constraints give rise to the volumetric contributions to the stress tensor. For the micro-free (a) and passivated (c) boundary conditions, yield occurs at $t := t_Y \approx 0.38$ s when $|\operatorname{dev} \boldsymbol{\sigma}| = Y$ (the initial yield stress). The onset of yielding at point P is delayed when micro-hard boundary conditions are imposed on the upper surface. Unsurprisingly, the presence of Dirichlet boundary conditions on the plastic strain changes the global response as the residual expression (6.2) now contains additional constraints. As seen in Fig. 8(b) the amount of hardening is minimal. The hardening is linear for the micro-free problem but is more complex for the micro-hard and passivated boundary conditions due to the contribution of the higher-order terms. Elastic unloading occurs at the onset of load stage B–C.

The yield stress, that is, the stress at which global behaviour undergoes the transition from elastic to elastic-plastic, is determined automatically as a result of the perturbed dissipation function used in the computations. Thus this approach allows the yield stress to be obtained despite a closed-form expression not being available, as discussed in Section 5.2.

For the passivation problem (c), the microscopic Dirichlet constraints on the plastic strain evolution are imposed at $t_{\text{pass}} > t_Y$. The evolution of the stress state at point P shows that the pre-passivation micro-free response transforms to a micro-hard response post-passivation. *This transition occurs elastically.* This is the phenomenon is referred to in [8] as an elastic gap. The system evolves to the curve corresponding to the micro-free boundary condition elastically, which may be interpreted as the most efficient route.

The analysis is earlier sections does not allow for a closed-form expression for the yield surface. This can however be explored numerically with reference to the stress response in σ_{11}–σ_{33} space, as shown in Fig. 9. Although not indicated, the micro-free response is identical to that obtained using a classical return mapping algorithm (closest-point projection) at the level of the

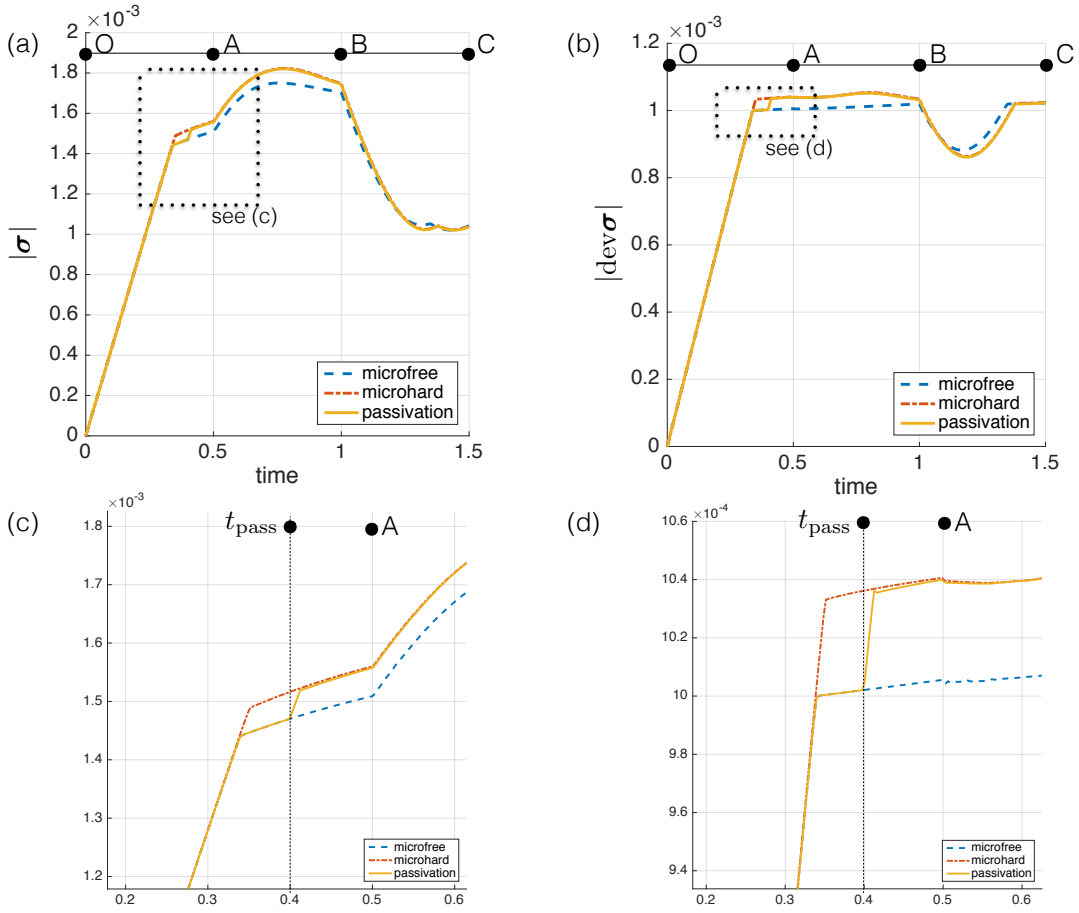

Figure 8: The evolution of (a) the Cauchy stress and (b) the Cauchy stress deviator at point P for the various boundary conditions. The various load stages are also indicated.

integration point for the non-gradient, rate-independent J_2 plasticity problem. This confirms that the global formulation based on a micro-force balance is essentially equivalent to the local formulation in the absence of gradients. It also confirms that for the micro-free condition the choice of a primal formulation with the dissipation function D_2 is equivalent to the dual problem with a von Mises yield surface. The yield surface for the micro-free problem in Fig. 9 can thus be seen as the von Mises yield surface corresponding to the classical problem.

The yield surface for the micro-hard problem is expanded relative to the micro-free one, consistently with the elastic gap transition reported earlier. Furthermore, due to the gradient contributions to the hardening, the expansion is not uniform. The yield surface for the passivated problem is on the micro-free surface until $t = t_{\text{pass}}$, after which it moves elastically to the micro-hard one.

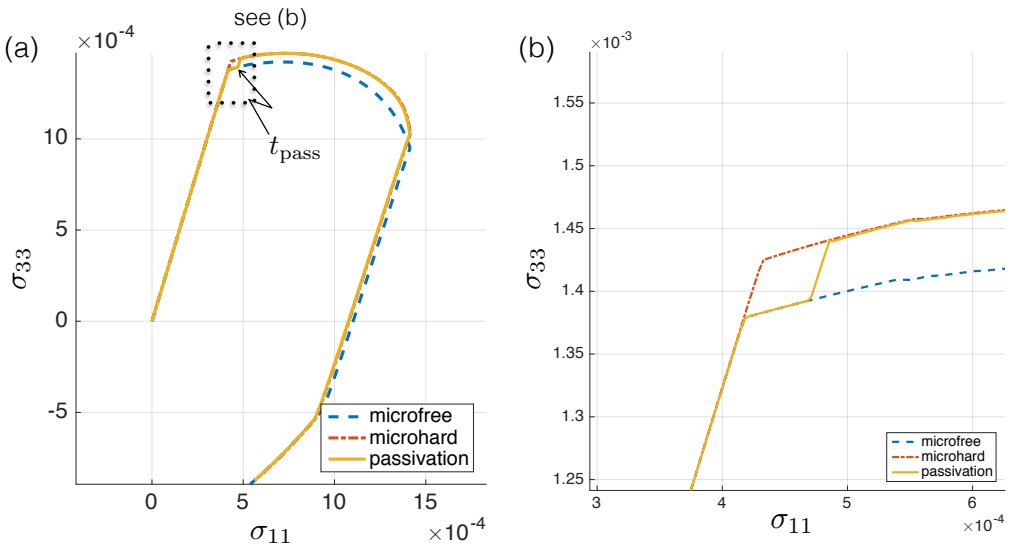

Figure 9: The evolution of the Cauchy stress components σ_{11} and σ_{33} for the various boundary conditions.

6.2 Extension of a micro-rod

Consider a rod having radius 25 µm and length $L = 50$ µm, and subjected to a prescribed displacement in the axial direction of 0.5 µm applied to the upper and lower faces with normals $\boldsymbol{e}_3$ and $-\boldsymbol{e}_3$, respectively. The curved side is traction-free. Due to symmetry, only the upper quarter of the rod is modelled as shown in Fig. 10. The prescribed displacement is imposed incrementally over 0.5 s. The response of the system at a material point labelled A and located at $[0, 0, 12.5]$ µm is recorded. The length scale, unless otherwise stated, is $l = 0.2L$. The domain is discretized using 6527 elements.

As in the previous example, the consequences of choosing different microscopic boundary conditions on the upper boundary of the domain, denoted Γ_{u}, are investigated. The curved side is at all times micro-traction free. Passivation occurs at $t_{\text{pass}} = 0.25$ s which is well into the plastic range.

The response at point A for the various choices of the microscopic boundary conditions on Γ_{u} is shown in Fig. 11. The relation between the magnitudes of the Cauchy stress and the strain, shown in Fig. 11(a), clearly contain the same features discussed in the previous example: an increase in the perceived yield strength for the micro-hard condition and an elastic gap for the passivation problem. Furthermore, the size of the elastic gap increases with increasing length scale. This relation between the size of the elastic gap and the length scale was also observed in [8].

The evolution of the quantity $\phi := |\mathsf{S}|/Y$, which corresponds to the classical yield function, is

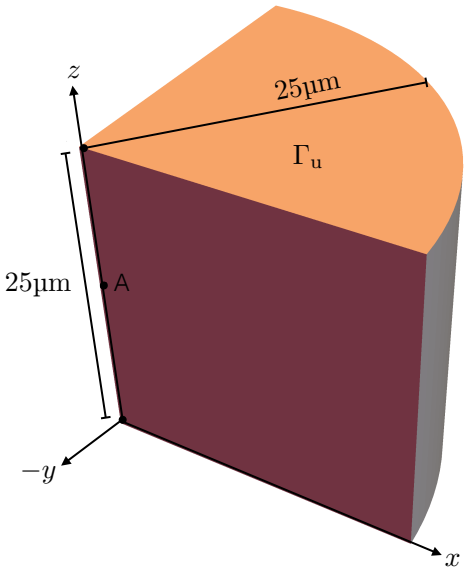

Figure 10: Computational domain for the problem of the extension of a rod.

shown in Fig. 11(b). As expected, ϕ is in the range $0 < \phi < 1$ in the elastic region, and $\phi = 1$ during plastic flow for all microscopic boundary conditions. The elastic gap at $t = t_{\text{pass}} = 0.25$ s is also clearly indicated for the passivation problems as ϕ drops below unity.

The evolution of the stress in σ_{11}–σ_{22}–σ_{33} space is shown in Fig. 11(c). For the micro-free condition, the stress state is uniaxial with σ_{33} the only non-zero stress component. The stress state remains at the point on the yield surface where initial yield occurred. The stress state is spatially uniform throughout the specimen and there are no plastic strain gradients present.

For the micro-hard boundary condition the stress evolves symmetrically in the σ_{11} and σ_{22} directions post yield. The micro-hard boundary condition constrains all components of the plastic strain, thereby inducing a stress response in directions other than that of the loading. Microscopic Dirichlet conditions on the plastic strain result in plastic strain gradients and Cauchy stresses in directions other than the loading direction. The yield surface for the passivation problem is identical to that of the micro-free problem prior to passivation. The stress state at the point of passivation will have only a σ_{33} component. Upon passivation, the elastic gap occurs. For the larger length scale of $l = 0.4L$ the yield surface appears to increase above the micro-hard one. It should be noted that post-passivation, the stress components plotted are no longer the principal stress components.

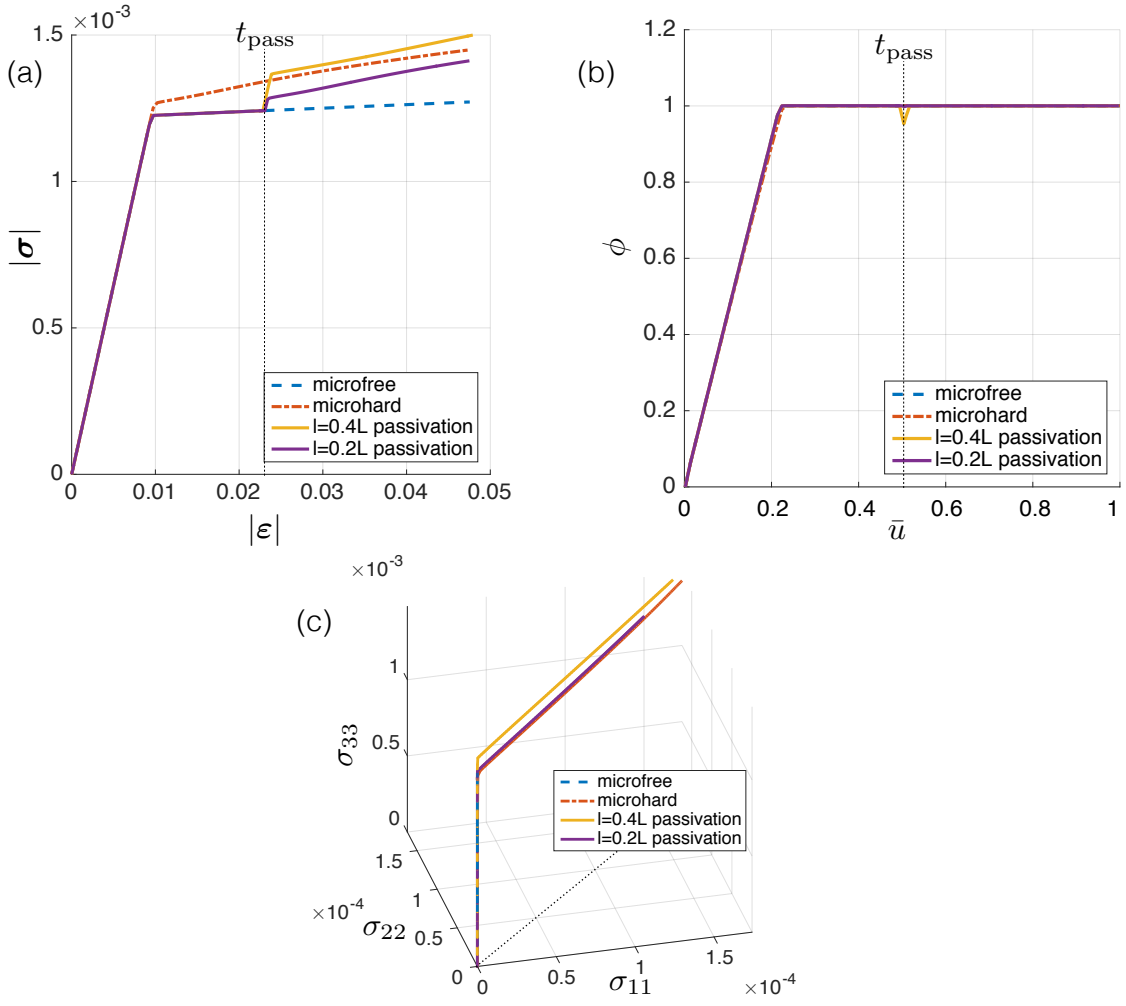

Figure 11: The evolution of the state at material point A for the rod extension problem for various microscopic boundary conditions and different length scales. The relation between $|\boldsymbol{\sigma}|$ and $|\boldsymbol{\varepsilon}|$ is shown in (a). The evolution of the canonical yield function ϕ and the Cauchy stress are shown in (b) and (c), respectively. The curve corresponding to the micro-hard boundary condition is for the length scale $\ell = 0.2L$.

7 Concluding remarks

A theoretical and computational investigation has been carried out of a dissipative model of rate-independent strain-gradient plasticity, that is, one in which gradient terms are accounted for only in the flow relation. The global nature of the flow relation, previously reported in [20], is reiterated. The most appropriate and effective approach to formulating the flow relation is through the use of a dissipation function; this form of the relation is especially useful in the context of numerical investigations. Dual formulations in terms of the yield function and a

normality relation have been approached using the tools of convex analysis. It is not possible, using conventional tools, to invert the flow relation to obtain the yield surface corresponding to the global dissipation function. This objective has been investigated further in the context of the fully discrete problem, for which an upper bound to the elastic region is found.

The numerical investigation casts further light on the response using the dissipative theory in situations of non-proportional loading due to passivation. Post-yield behaviour has been investigated. The elastic gap reported in [8] and analyzed in [12] has been observed in situations in which passivation has been imposed. It has been possible to interpret the gap mathematically, using the expression for the yield function as a maximum, taken over all admissible plastic strain increments, of a function involving the dissipation: the vector of admissible increments is necessarily smaller in dimension following passivation, and the corresponding maximum may therefore be smaller than that in the step preceding passivation. The elastic gap has also been observed to constitute an "efficient" transition from a stress-strain curve corresponding to a micro-free boundary condition, to that which is obtained assuming micro-hard boundary conditions.

The dissipative model of strain-gradient plasticity is mathematically well posed [20]. The presence of the elastic gap, at least in the case of a change of boundary conditions achieved through passivation, is indisputable from theoretical and numerical perspectives, as has been demonstrated here and in the works by Fleck, Hutchinson and Willis. The actual physical response is one that awaits experimental investigation, as has been emphasized by these authors. Such testing would clarify the predictive nature of the theory: for example, as suggested in [12], as a theory in which small plastic deformation is approximated as zero plastic deformation.

8 Acknowledgements

BDR acknowledges many helpful discussions on the topic of this paper with JW Hutchinson. The work reported in this paper was carried out with support through the South African Research Chair in Computational Mechanics to BDR and ATMcB. This support is gratefully acknowledged. PS acknowledges support through the Collaborative Research Center 814.

References

[1] Aifantis, E.C. (1984). On the microstructural origin of certain inelastic models. J. Engng Mat.Tech. **106** 326–330.

[2] Anand, L., Gurtin, M.E., Lele, S.P. and Gething, C. (2005). A one-dimensional theory of strain-gradient plasticity: Formulation, analysis, numerical results. J. Mech. Phys. Solids

53(8) 1789–1826

[3] Bardella, L. and Panteghini, A. (2015). Modelling the torsion of thin metal wires by distortion gradient plasticity. J. Mech. Phys. Solids **78** 467–492.

[4] Chiricotto, M. and Giacomelli, L. and Tomassetti, G. (2016). Dissipative scale effects in strain-gradient plasticity: the case of simple shear. SIAM J. Appl. Math. **76**(2) 688–704.

[5] Ekeland, I. and Temam, R. (1976). Convex Analysis and Variational Problems. North-Holland, Amsterdam.

[6] Evans, A.G. and Hutchinson, J.W. (2009). A critical assessment of theories of strain gradient plasticity. Acta Materialia **57** 1675–1688.

[7] Fleck, N.A. and Hutchinson, J.W. (2001). A reformulation of strain gradient plasticity. J. Mech. Phys. Solids **49** 2245–2271.

[8] Fleck, N.A., Hutchinson, J.W. and Willis, J.R. (2015). Strain-gradient plasticity under non-proportional loading. Proc. R. Soc **A 470** 20140267.

[9] Fleck, N.A., Hutchinson, J.W. and Willis, J.R. (2015). Guidelines for constructing strain gradient plasticity theories. J. Appl. Mech. **82** 071002-1-10.

[10] Fleck, N.A. and Willis, J.R. (2009). A mathematical basis for strain-gradient plasticity - Part I: Scalar plastic multiplier. J. Mech. Phys. Solids **57** 151–177.

[11] Fleck, N.A. and Willis, J.R. (2009). A mathematical basis for strain-gradient plasticity - Part II: Tensorial plastic multiplier. J. Mech. Phys. Solids **57** 1045–1057.

[12] Fleck, N.A. and Willis, J.R. (2015). Strain gradient plasticity: energetic or dissipative? Acta Mech. Sinica **31** 465–472.

[13] Gao H., Huang Y. and Nix W.D. 1999. Mechanism-based strain gradient plasticity ? I. Theory. J. Mech. Phys. Solids **47** 1239–1263.

[14] Gao H., Huang Y., Nix W.D. and Hutchinson J.W. (1999). Modeling plasticity at the micrometer scale, Naturwissenschaften **86** 507–515.

[15] Gudmundson, P. (2004). A unified treatment of strain gradient plasticity. J. Mech. Phys. Solids **52** 1379–1406.

[16] Gurtin, M.E., Anand, L. (2005). A theory of strain-gradient plasticity for isotropic, plastically irrotational materials. Part I: small deformations. J. Mech. Phys. Solids **53** 1624–1649.

[17] Han, W. and Reddy, B.D. (2013). Plasticity: Mathematical Theory and Numerical Analysis. Springer, New York and Berlin.

[18] Korelc, J. (2002). Multi-language and multi-environment generation of nonlinear finite element codes. Engng Comp. **18**(4) 312–327.

[19] Panteghini, A. and Bardella, L. (2016). On the Finite Element implementation of higher-order gradient plasticity, with focus on theories based on plastic distortion incompatibility. Comput. Methods Appl. Mech. Engrg. **310** 840–865.

[20] Reddy, B.D. (2011). The role of dissipation and defect energy in variational formulations of problems in strain-gradient plasticity. Part 2: single-crystal plasticity. Continuum Mech. Thermodyn. **23** 547–549.

[21] Reddy, B.D., Ebobisse, F. and McBride, A.T (2008). Well-posedness of a model of strain gradient plasticity for plastically irrotational materials. Int. J. Plast. **24** 55–73.

[22] Rockafellar, R.T. (1970). Convex Analysis. Princeton University Press, Princeton, N.J.